

# SUPPRESSION OF WAKEFIELD INDUCED ENERGY SPREAD INSIDE AN UNDULATOR THROUGH CURRENT SHAPING \*

J. Qiang<sup>†</sup> and C.E. Mitchell, LBNL, Berkeley, CA 94720, USA

## Abstract

Wakefields from resistive wall effects inside an undulator can cause significant growth of the beam energy spread and limit the performance of x-ray FEL radiation. In this paper, we propose a method to mitigate such wakefield-induced energy spread by appropriately conditioning the electron beam current profile. Numerical examples and potential applications will also be discussed.

## INTRODUCTION

Wakefields such as the resistive wall wakefield and the surface roughness wakefield inside an undulator can cause significant electron beam energy loss and energy spread growth. Such energy loss inside an undulator can heat the vacuum pipe and also induce energy variation along the bunch length that will limit the performance of the undulator and the quality of the final FEL radiation. For a seeded FEL, such energy variation will increase the bandwidth of the radiation. If the relative energy variation inside the beam is larger than the FEL Pierce parameter, the coherent radiation from part of the beam can even be suppressed. In previous studies, the relative energy change due to the resistive wall wakefield was calculated for a room-temperature normal conducting LCLS undulator using a double-horn beam distribution from the LCLS linac [1]. The resistive wall heating of the undulator from the wakefield was also calculated for a high repetition rate FEL [2]. In this paper, we report on a method to suppress the energy variation along the bunch length induced by the resistive wall wakefield inside an undulator through longitudinal current profile shaping. A similar method was previously proposed to suppress the emittance growth driven by coherent synchrotron radiation inside a bunch compressor chicane [3].

The total wakefield-induced energy loss per meter from a single bunch of the electron beam inside an undulator is given by

$$E_{tot} = \int_{-\infty}^{\infty} E_w(z)\rho(z)dz \quad (1)$$

where

$$E_w(z) = \int_{-\infty}^z w(z-z')\rho(z')dz' \quad (2)$$

Here  $w(z)$  is the single-particle wake function for an electron inside the undulator,  $z$  and  $z'$  denote the electron longitudinal coordinate with respect to the head of the beam

(on the left),  $\rho(z)$  is the electron longitudinal line charge density,  $E_w(z)$  is the energy loss per meter per Coulomb along the beam, and  $E_{tot}$  is the total energy loss per meter of the electron bunch. The power loss to the vacuum pipe per meter for a high repetition light source is given by the product of the repetition rate and the single bunch total energy loss (1). The rms energy spread per meter of the beam induced by such energy loss is given by

$$E_{rms} = \sqrt{\int_{-\infty}^{\infty} (E_w(z) - E_{tot})^2 \rho(z) dz} \quad (3)$$

The single-particle wake function used in (2) is related to the impedance [1] by

$$w(z) = \frac{2c}{\pi} \int_{-\infty}^{\infty} \text{Re}(Z(k)) \cos(kz) dz \quad (4)$$

where  $\text{Re}(Z(k))$  denotes the real part of the resistive wall impedance  $Z$  inside the undulator and  $c$  is the speed of light in vacuum.

## CONTROL OF ENERGY MODULATION INDUCED BY WAKEFIELD THROUGH CURRENT PROFILE SHAPING

For a given current profile, the wakefield-induced energy loss along the beam can be calculated using (2). This equation can also be used to control the energy variation along the beam by choosing an appropriate longitudinal current profile. For a given single-particle wake function  $w$  and a desired wakefield  $E_w$ , (2) defines an integral equation for the current profile  $\rho$ . Such an integral equation can be solved analytically or numerically for the desired current profile.

First, we consider the case when the resistive wall wake function can be approximated by an analytical resonator wake function of the form [1]:

$$w(z) = \frac{1}{\pi\epsilon_0 a^2} \exp(-z/\sigma_l) \cos(\omega z) \quad (5)$$

where  $\sigma_l = 4c\tau$ ,  $\omega = \sqrt{2k_p/a}$ ,  $k_p = \sqrt{Z_0\sigma/(c\tau)}$ ,  $\tau$  is the pipe material relaxation time,  $\sigma$  is the pipe material DC conductance,  $a$  is the pipe radius,  $Z_0$  is the vacuum impedance,  $c$  is the speed of light in vacuum, and  $\epsilon_0$  is the vacuum permittivity. To induce a uniform (step function) energy loss along the beam, with the above resonator wake function, the electron line density distribution can be obtained by solving the integral equation (2) using a Laplace transform method. The resulting density distribution is

$$\rho(z) = \rho_0[\delta(z) + \frac{H(z)}{\sigma_l} + \sigma_l\omega^2(1 - e^{-z/\sigma_l})H(z)] \quad (6)$$

\* Work supported by the U.S. Department of Energy under Contract No. DE-AC02-05CH11231 using computing resources at the NERSC.

<sup>†</sup> jqiang@lbl.gov

where  $H(z)$  is the step function defined by  $H(z) = 1$  for  $z$  between 0 and the bunch length  $L$ , and  $\delta(z)$  is the Dirac-delta function. The  $\delta$  function at  $z = 0$  (the head of the beam) is due to the discontinuity of the wakefield at that point. The general solution to the integral equation (2) for the line density distribution  $\rho$  with the resonator wake function (5) and the wakefield  $E_w(z)$  can be written as:

$$\rho(z) = \rho_0 \left[ E'_w(z) + \frac{E_w(z)}{\sigma_l} + \omega^2 \int_0^z E_w(z') e^{-(z-z')/\sigma_l} dz' \right] \quad (7)$$

To induce a linear energy loss along the beam, i.e. the wakefield  $E_w(z) = \alpha z$ , the longitudinal current profile is obtained as:

$$\rho(z) = \rho_0 \alpha \left[ 1 + \frac{z}{\sigma_l} + \sigma_l^2 \omega^2 \left( \frac{z}{\sigma_l} - 1 + e^{-z/\sigma_l} \right) \right] \quad (8)$$

Next, we consider the case of the resistive wall wakefield inside a normal conducting undulator. For a short electron beam inside the undulator, the AC conductivity becomes important. The conductivity of the pipe material is no longer a constant but responds to oscillations in the applied field. The AC resistive wall impedance is given in reference [1] as:

$$Z(k) = \frac{Z_0}{2\pi a^2} \left[ \frac{1}{s_0^2} \sqrt{\frac{t_\lambda}{\Gamma k^2}} (i\sqrt{1+t_\lambda} + \text{sgn}(k)\sqrt{1-t_\lambda}) - \frac{ik}{2} \right]^{-1} \quad (9)$$

where

$$t_\lambda = \frac{|ks_0|\Gamma}{\sqrt{1+(ks_0\Gamma)^2}} \quad (10)$$

where  $\Gamma = \tau c/s_0$ ,  $s_0 = (\frac{2a^2}{Z_0\sigma})^{1/3}$  is the characteristic length inside the pipe,  $\tau$  is the relaxation time,  $\sigma$  is the pipe material DC conductance,  $a$  is the pipe radius,  $Z_0$  is the vacuum impedance, and  $c$  is the speed of light in vacuum. From the above impedance, the single-particle wake function can be calculated numerically using (4). Given numerical values of the wake function on discrete grid points along the length of the beam, the integral equation (2) has to be solved numerically for a given distribution of the wakefield  $E_w$ . At each discrete location  $z_i = ih_z$  for  $i = 1, \dots, N$ , the wakefield integral can be approximated as:

$$E_{wi} = h_z \sum_{j=1}^i \rho_{j-1/2} w_{i-(j-1/2)} \quad (11)$$

where  $L = Nh_z$  and  $h_z$  is the grid size. Approximating the wake function  $w_{i-(j-1/2)} = (w_{i-j} + w_{i-j+1})/2$ , we obtain

$$E_{wi} = h_z \sum_{j=1}^i \rho_{j-1/2} (w_{i-j} + w_{i-j+1})/2 \quad (12)$$

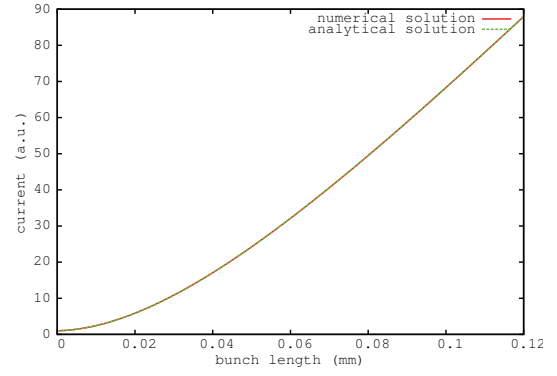


Figure 1: A comparison of the current profile from the numerical scheme (red) and the analytical solution (green) for a linear wakefield with the resonator wake function (the head of the beam is to the left).

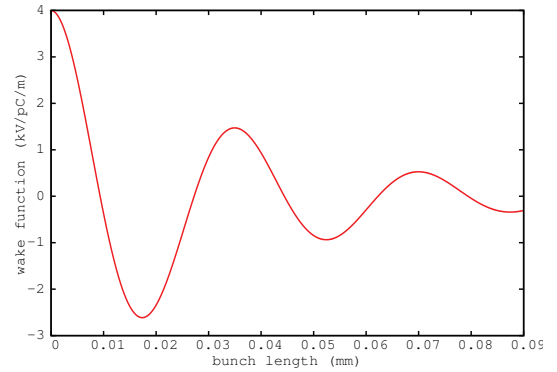


Figure 2: Longitudinal wake function inside the normal conducting undulator (Cu) with an aperture size of 6 mm (the head of the beam is to the left).

The above set of algebraic equations can be solved for the values  $\rho_{j-1/2}$  using a forward substitution method. These solutions can then be used to find the solutions  $\rho_j$  at each grid point using interpolation. As a test of the above numerical scheme, we calculate the current profile needed to generate a linear wakefield with the resonator wake function (5). The numerical solution is shown together with the analytical solution (8) in Fig. 1. It is seen that the numerical solution agrees with the analytical solution very well.

Using the above AC normal conducting impedance model, we calculate the single-particle wake function (4) in a normal conducting Cu undulator with 6 mm aperture size. This wake function is shown in Fig. 2. Using this wake function, we calculate the current profile needed to generate a uniform energy loss along the beam inside the normal conducting undulator. The resulting current profile is shown in Fig. 3. It is seen that the current profile from the numerical solution has a very large spike at the head of the beam ( $z = 0$ ) as shown in the zoom-in plot in the figure. This large spike is a numerical approximation to the true delta function solution at the origin  $z = 0$  due to the discontinuity of the wakefield at the origin for a step function wakefield. This delta function solution is also

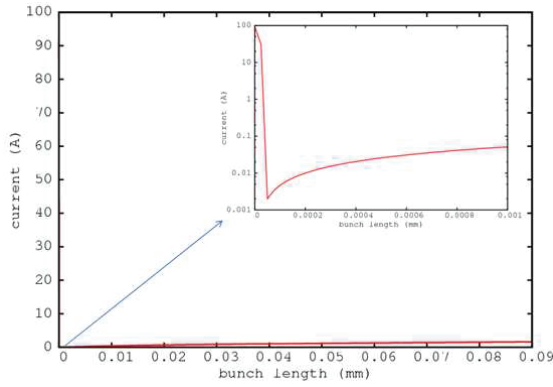


Figure 3: Current profile for a step function wakefield inside the normal conducting undulator (the head of the beam is to the left).

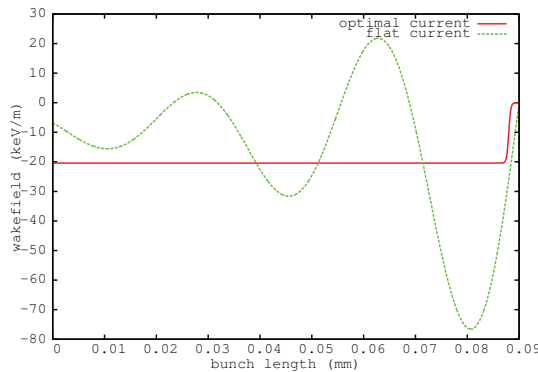


Figure 4: Wakefields from the desired logistic function (red) and from a flat-top current profile (green) inside the normal conducting undulator (the head of the beam is to the right).

present in the analytical solution (6) with a resonator wake function. To avoid the delta function in the current profile resulting from the discontinuity of the wakefield, instead of using a step function wakefield, we assume a logistic function wakefield given by:

$$E_w(z) = \frac{A}{1 + e^{-(z-z_{mid})/z_{scale}}} - E_{w0} \quad (13)$$

where  $A$  is a normalizing constant depending on the total charge of the beam,  $z_{mid}$  and  $z_{scale}$  are constants controlling the range of the ramping region before entering into the region of flat wakefield, and  $E_{w0}$  is the value of the logistic function at  $z = 0$ . This desired energy loss along the beam together with the wakefield generated by a flat-top current profile is given in Fig. 4 assuming a total bunch charge of 300 pC and  $z_{mid} = 2 \mu\text{m}$ ,  $z_{scale} = 0.2 \mu\text{m}$ . There is only a small fast ramping region (less than  $5 \mu\text{m}$ ). Most of the beam has a flat uniform energy loss, while the energy loss from the uniform flat-top current profile shows a large oscillation. This large oscillation could cause broadening of the radiation bandwidth and even suppress the coherent radiation if the relative oscillation amplitude is larger than the

ISBN 978-3-95450-126-7

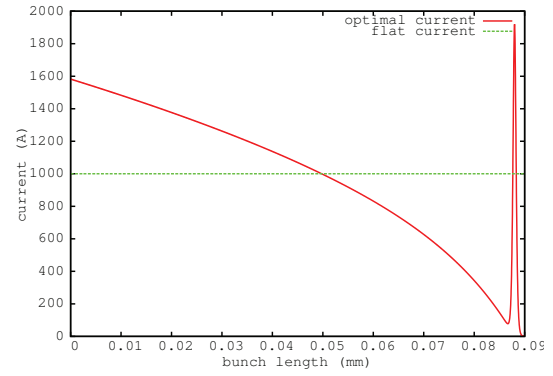


Figure 5: Current profiles for the desired logistic function wakefield inside the normal conducting undulator (red). The assumed flat-top step function current profile is also given (green) (the head of the beam is to the right).

FEL parameter. We calculated the current profile needed to generate the desired logistic function wakefield (13), and the results are shown in Fig. 5. The current profile shows a spike near the head of the beam and increases continuously towards the end of the beam.

As a third case, we consider the wakefield-induced energy loss inside a superconducting undulator. The AC resistive wall impedance (9) works well when the mean free path length ( $v_f \tau$ ) is smaller than the classical skin depth  $\delta_s$  given by

$$\delta_s = \sqrt{\frac{c}{2\pi\sigma k}} \quad (14)$$

where  $v_f$  is the Fermi velocity. In the situation of low temperature superconducting undulators, the above condition is not valid. This is also called the anomalous skin effect (ASE). The resistive wall impedance with the anomalous skin effect is given in reference [4] as

$$Z(k) = \frac{2Z_0(Ba)^{3/5}}{\pi a^2} \frac{\bar{k}^{2/3}}{1 + i(\sqrt{3} - 2\bar{k}^{5/3})} \quad (15)$$

where  $B = (\frac{\sqrt{3}}{16\pi Z_0} l/\sigma)^{1/3}$ ,  $\bar{k} = k(Ba)^{3/5}$  and  $l$  is the mean free path of the conducting electrons. The single-particle wake function for a  $Cu$  superconducting undulator with 6 mm aperture size is shown in Fig. 6. This wake function appears to be less oscillatory than the one in the normal conducting undulator. Fig. 7 shows the desired wakefield and the wakefield obtained from a flat-top uniform current profile with 300 pC charge inside the  $Cu$  superconducting undulator. The energy loss along the beam due to the resistive wall wakefield in the superconducting undulator is less than that in the normal conducting undulator. Fig. 8 shows the current profile needed to generate the desired logistic function wakefield (13). The current profile required to generate the wakefield (13) inside the superconducting undulator has a similar shape as that required inside the normal conducting undulator. The current spike inside superconducting undulator is smaller than the spike inside the

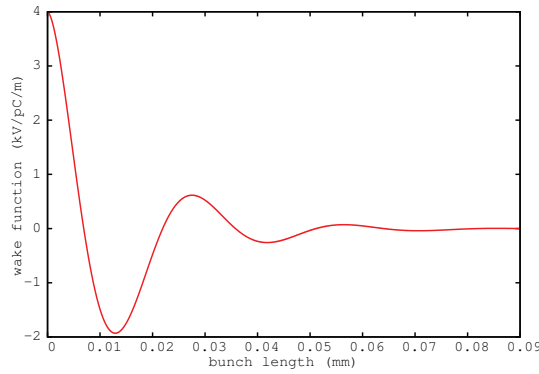


Figure 6: Longitudinal wake function inside the superconducting undulator (Cu) with an aperture size of 6 mm (the head of the beam is to the left).

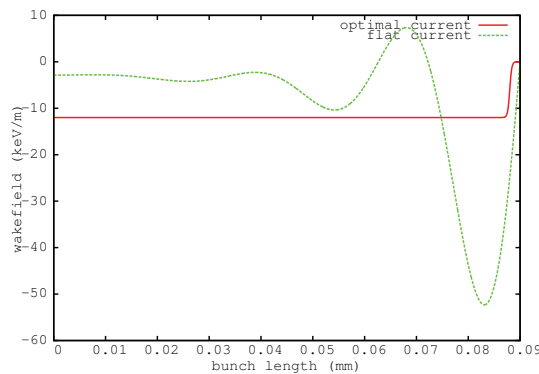


Figure 7: Wakefields from the desired logistic function (red) and from a flat-top current profile (green) inside the superconducting undulator (the head of the beam is to the right).

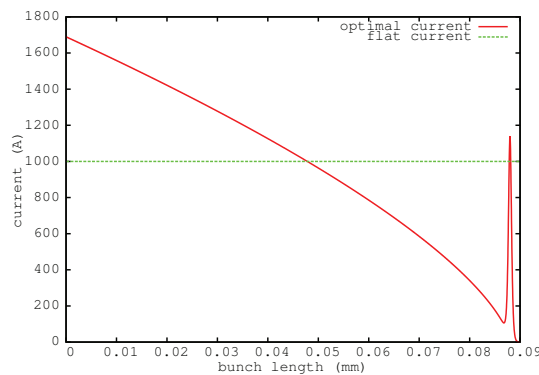


Figure 8: Current profiles for the desired logistic function wakefield inside the superconducting undulator (red). The uniform flat-top current profile is also given (green) (the head of the beam is to the right).

normal conducting undulator due to the fact that the single-particle wake function is less oscillatory in the superconducting undulator. Such a current spike near the head of the beam might be generated by using a nonlinear longitudinal phase space distribution near the beam head and passing through a bunch compressor.

### REFERENCES

- [1] K.L.F. Bane, “Resistive Wall Wakefield in the LCLS Undulator Beam Pipe,” SLAC-PUB-10707, Revised October 2004.
- [2] J. Qiang, J. Corlett, P. Emma, J. Wu, “Resistive wall heating of the undulator in high repetition rate FELs,” in Proceedings of IPAC 2012, p. 652 (2012).
- [3] C. Mitchell, J. Qiang, P. Emma, Phys. Rev. ST Accel. Beams 16, 060703 (2013).
- [4] B. Podobedov, Phys. Rev. ST Accel. Beams 12, 044401 (2009).